**Revista de Metalurgia**
January-March 2022, 58 (1), e213
ISSN-L: 0034-8570
https://doi.org/10.3989/revmetalm.213

# Investigation on dry sliding wear behavior of AA5083/nano-$Al_2O_3$ metal matrix composites

R. Suresh[a,*], Joshi Ajith G.[b], N.G. Siddeshkumar[c]

[a] Department of Mechanical and Manufacturing Engineering, M.S. Ramaiah University of Applied Sciences, Bengaluru, 560054, India

[b] Department of Mechanical Engineering, Canara Engineering College, Bantwal, Mangalore, 574219, India

[c] Department of Mechanical Engineering, Channabasaveshwara Institute of Technology, Gubbi, Tumkur, 572216, India

(*Corresponding author: sureshchiru09@gmail.com)

Submitted: 22 January 2022; Accepted: 11 March 2022; Available On-line: 30 March 2022

**ABSTRACT:** The tribological behavior of aluminum alloy (AA5083)/nano-$Al_2O_3$ metal matrix composites with varying reinforcement percentage of 2, 4, 6 and 8 wt.-% nano-$Al_2O_3$ particles was studied. The Al/nano-$Al_2O_3$ composites were prepared using a stir casting route. The scanning electron microscopy (SEM) images of prepared specimens suggested nearly uniform dispersion of nanoparticles in the Al matrix. Sliding wear behavior was studied using a pin-on-disc test rig. The plan of experiments was in accordance with Taguchi's L25 orthogonal array using three process parameters at five levels viz. reinforcement weight percentage, applied load and sliding distance. The obtained results reveal that nano-particles reinforced composites exhibited better wear resistance. While the main effects plot suggested that wear increases with an increase in the load, the sliding distance and decreases with an increase in the reinforcement percentage. The analysis of variance (ANOVA) illustrated that the sliding distance was the most significant contributing parameter. The worn surface morphology of the specimen tested under the highest load condition revealed the occurrence of abrasive wear phenomenon.

**KEYWORDS:** ANOVA; Metal matrix composites; Nano-$Al_2O_3$; Sliding wear; Taguchi

Citation/Citar como: Suresh, R.; Ajith G.J.; Siddeshkumar, N.G. (2022). "Investigation on dry sliding wear behavior of AA5083/nano-$Al_2O_3$ metal matrix composites". *Rev. Metal.* 58(1): e213. https://doi.org/10.3989/revmetalm.213

**RESUMEN:** *Investigación del comportamiento al desgaste por deslizamiento en seco de materiales compuestos de matriz metálica AA5083/NANO-$Al_2O_3$.* Se ha estudiado el comportamiento tribológico de materiales compuestos de matriz metálica de aluminio (AA5083)/nano-$Al_2O_3$ con un porcentaje de refuerzo variable de 2, 4, 6 y 8% en peso de partículas de nano-$Al_2O_3$. Los compuestos Al/nano-$Al_2O_3$ se prepararon utilizando una ruta de colada por agitación. Las imágenes de microscopía electrónica de barrido (MEB) de los materiales sugirieron una dispersión casi uniforme de las nanopartículas en la matriz de Al. El comportamiento al desgaste por deslizamiento se estudió utilizando un banco de pruebas pin-on-disc. El plan de experimentos tuvo como referencia la matriz ortogonal L25 de Taguchi utilizando tres parámetros de proceso en cinco niveles, a saber, porcentaje en peso de refuerzo, carga aplicada y distancia de deslizamiento. Los resultados obtenidos revelan que los mate-

riales compuestos reforzados con nanopartículas presentan una mejor resistencia al desgaste. Mientras que la gráfica de efectos principales sugirió que el desgaste aumenta con un aumento en la carga, la distancia de deslizamiento y disminuye con un aumento en el porcentaje de refuerzo. El análisis de varianza (ANOVA) ilustró que la distancia de deslizamiento fue el parámetro más significativo. La morfología de la superficie desgastada del espécimen probado, bajo la condición de carga más alta, reveló la ocurrencia de un fenómeno de desgaste abrasivo.

**PALABRAS CLAVE:** ANOVA; Material Compuesto de Matriz metálica; Nano-$Al_2O_3$; Desgaste por Deslizamiento; Taguchi

**ORCID ID:** R. Suresh (http://orcid.org/0000-0002-6956-9751); Joshi Ajith G. (http://orcid.org/0000- 0002-5867-8186); N.G. Siddeshkumar (http://orcid.org/0000-0002-8212-1804)

## 1. INTRODUCTION

Conventional engineering materials possess superior individual characteristics. However current engineering applications demand tailored characteristics such as specific modulus and specific strength. Metal matrix composites (MMCs) with hard particulate reinforcements are recommended to address such issues and to cater to the need for advanced industrial requirements (Kumar *et al.*, 2018; Cavdar *et al.*, 2020). MMCs find a wide range of applications comprising automotive, aerospace, machine components due to their superior wear resistance, high-temperature stability, specific strength and stiffness (Basavarajappa *et al.*, 2007). Commonly used reinforcements in MMCs are $Al_2O_3$, $SiO_2$, TiC, $B_4C$, SiC, etc., particles yielding considerable enhancement of physical, thermal and mechanical properties. Further, soft reinforcements such as graphite, $MoS_2$, $Cu_2S$ are incorporated to develop self-lubricating materials (Pang *et al.*, 2018). Aluminum (Al) alloys are widely used as suitable materials for automotive and aerospace applications to meet the demand for low-density alloys (Çömez, 2021). However, their strength and tribological characteristics are major concerns (Shivakumar *et al.*, 2015). Aluminum-based MMCs (AMMCs) are widely used to overcome such limitations. AMMCs possesses higher strength, stiffness, wear-resistance and considerably lower density. They found applications such as sliding contacts like clutch, brake shoes, bearings (Srivyas and Charoo, 2018).

In the last decade, efforts are being made to study the effect of nanosized reinforcements on the performance of MMCs. Consequently, the advantage of particulate reinforcement has been enhanced through a reduction in its size to nano (Casati and Vedani, 2014). Nanoscale reinforcements have shown significant contribution towards enhancement of composite properties owing to improved particle-dislocation interaction, due to size reduction (Shivakumar *et al.*, 2015). The addition of a small amount of nanoparticles results in better strength and wear properties of MMCs compared to properties of 15% micro-particulate reinforced MMCs (Padhi and Kar, 2011; Kok, 2005). Thus, they are emerging as promising materials to cater to the needs of industrial applications (Kumar and Chaudhari, 2014; Ezatpour *et al.*, 2014). Besides, homogeneity in the dispersion phase is the primary aspect of improving the characteristics of AMMCs.

Nanoparticles have a significant effect on fracture morphology leading to brittle fracture properties. Also, nano-particle reinforcement significantly enhances microstructure, wear and hardness characteristics of AA5250 alloy (Moustaf *et al.*, 2021; Essa *et al.*, 2021). Kim *et al.* (2007) have reported that CNT/Cu nanocomposites have shown better wear resistance with an increase in CNT volume fraction through reduced delamination of Cu. Tu *et al.* (2003) stated nano-$TiB_2$ reinforcement in copper has improved wear resistance. While reduced local plastic deformation was observed with a higher content of $TiB_2$. The use of Al in tribological applications has increased with the evolution of AMMCs and extended with nano reinforcements. Mobasherpour *et al.* (2013) fabricated aluminum nanocomposites of Al7075 alloy and $Al_2O_3$ synthesized using ball milling. Characterization of composite powders was carried out using SEM and XRD which showed particle sizes in the range 30 – 50 nm. The composites prepared were found to have higher hardness and ultimate tensile strength also increased with an increase in the percentage of $Al_2O_3$. El-kady *et al.* (2015) and Ray *et al.* (2015) have depicted that $Al_2O_3$ incorporated nano-MMCs exhibit better tribological behavior compared to Al alloys. Jeyasimman *et al.* (2014) have shown that Al 6061–2 wt.-% TiC nanocomposite exhibited approximately four times higher hardness compared to microcrystalline Al alloy. Narasimha Murthy *et al.* (2012) have processed nano-flyash/Al composites through the ultrasonic cavitation route and attained improved compressive strength and hardness. Ma *et al.* (2017) studied the influence of Nano $Al_2O_3$ with Al-12Si on mechanical properties and strengthening mechanisms. Higher hardness and strengths were obtained for composite with 5 wt.-% of $Al_2O_3$ reinforcement. The mechanism of thermal mismatch strengthening has a significant effect on the strengthening of composites. Ezatpour *et al.* (2016) have shown that the distribution of nanoparticles in the Al matrix was improved with the injection of pure argon gas during hot extrusion. It was confirmed through SEM and HRTEM observations. Somani and Gupta (2021) that increase in % of reinforcement of nano particles in MMCs has resulted in significant

reduction of wear rate. It was attributed with abrasive wear mechanism characterized by ploughing, smearing and so on. Besides, there exists a threshold value of nano-particle reinforcement percentage, over that percentage, reinforcement leads to particulate agglomeration and greater porosity. Subsequently, it results in the deterioration of mechanical properties (Raturi *et al.*, 2017). Hence, the optimization of the reinforcement percentage and process parameters is highly significant to attain lucrative MMCs for applications.

Azimi *et al.* (2015) attempted to optimize process parameters using Taguchi statistical analysis for achieving better mechanical properties during the fabrication of Al/5%-TiC nano-composites. Various researchers (Ekka *et al.*, 2014; Singh *et al.*, 2015; Idrisi *et al.*, 2018) have employed statistical analysis techniques for studying the dry sliding wear behavior of metal matrix nanocomposites (MMNCs) and establish regression models to predict wear rate. Gargatte *et al.* (2013) have investigated the wear behavior of SiCz reinforced AA 5083 aluminum alloy using an L9 orthogonal array. ANOVA results revealed that sliding speed has the highest effect, while the reinforcement amount has a certain effect on wear rate. Mousavian *et al.* (2021) has successfully fabricated nano-SiC in Al matrix through a novel method comprising a combination of stir casting and semisolid extrusion techniques.

The characteristics of nanocomposites and their suitability in various advanced technologies are still being explored. The study on Al5083 based nanocomposites is rather limited available. Al 5083 is a magnesium-based non-heat treatable alloy, widely used in harsh environments such as seawater and industrial chemical environments. Its usage has increased nowadays in many engineering applications. Thus, the present work aims to investigate the dry sliding wear behavior of AA5083 reinforced with nano $Al_2O_3$ MMCs. The effect of nano-particulate reinforcement, normal load, and sliding distance on wear behavior was investigated. Further, there is scope for statistical modeling and analysis of wear of Al-based nano-MMCs. Hence, the current study attempts to identify significant factors influencing wear and to present the regression model for predicting wear within the studied range of factors.

## 2. MATERIALS AND EXPERIMENTATION

### 2.1. Fabrication of Nano-MMCs

Al 5083 was used as matrix material in the present work and its composition is indicated in Table 1. Nano-$Al_2O_3$ particles supplied by Sigma-Aldrich (India) was used as reinforcement and their size was 40 nm. The packets of approximately 8 gm of particles were prepared using aluminum foils. During the processing of packets, packed particles in aluminum foils were preheated up to 580 °C for 2 hours to eliminate the absorbed moisture. The stir casting method was employed for the fabrication of Al5083/$Al_2O_3$ nanocomposites. This method has proved to be very successful in the preparation of nano-MMCs at relatively lower cost and simple method (Ekka *et al.*, 2015). The method used for processing both alloy and composite. The packets were added to melt during the stir casting process. The stirrer is rotated before and after the addition of particles to achieve uniform distribution in the melt. During stirring, the addition of a small amount of magnesium (0.5 wt.-%) strips was done to enhance the wettability of particles. Later, the molten mix was poured into a preheated mold box (heated to 800 °C) and castings were removed after solidification to obtain the cylindrical specimen. The percentage of nano-$Al_2O_3$ particle reinforcement was varied as 2 wt.-%, 4 wt.-%, 6 wt.-% and 8 wt.-% to prepare 4 different Al/nano-$Al_2O_3$ MMCs.

### 2.2. Wear test

The dry sliding wear behavior of prepared composites was studied with the help of a pin-on-disc test rig (Manufactured by DUCOM®) under ambient conditions. Specimens were carefully mounted on a steel disc and adjusted to ensure perpendicular-

Table 1: Chemical composition of aluminum alloy AA 5083

| Element | Fe | Si | Cu | Mg | Mn | Ti | Zn | Cr | Al |
|---|---|---|---|---|---|---|---|---|---|
| wt.-% | 0.4 | 0.4 | 0.1 | 4.0-4.9 | 0.4-1.0 | 0.15 | 0.25 | 0.05-0.25 | Balance |

Table 2: Wear test parameter with levels

| Levels | Specimen Material | Applied Load (N) | Sliding Distance (m) |
|---|---|---|---|
| **1** | AA5083 | 4.905 | 1000 |
| **2** | AA5083+2% nano-$Al_2O_3$ | 9.810 | 2000 |
| **3** | AA5083+4% nano-$Al_2O_3$ | 14.715 | 3000 |
| **4** | AA5083+6% nano-$Al_2O_3$ | 19.620 | 4000 |
| **5** | AA5083+8% nano-$Al_2O_3$ | 24.525 | 5000 |

ity. The counter-face disc rotated against specimens was EN 32 grade steel with 65 HRC. The samples were machined into cylindrical pins of 8 mm diameter and 30 mm length with ground ends as per the ASTM G99 (2017). The wear was recorded through the data acquisition system as a function of pin height reduction. The sliding wear test was conducted at a constant sliding speed of 13.33 $m \cdot s^{-1}$, while other parameters are shown in Table 2. The possible wear mechanism was studied using worn surface morphology through field emission scanning electron microscopy (FESEM) images.

### 2.3. Microstructure analysis and hardness

The particulate dispersion study and microstructural analysis of prepared specimens were carried out using FESEM images. Standard metallographic techniques were followed to prepare specimens for microstructure and hardness study. Figure 1 to 4 presents SEM micrographs of AA5083 reinforced with 2, 4, 6 and 8 wt.-% of nano-$Al_2O_3$ respectively. The agglomeration phenomenon of nano-particles in prepared composites was minimum in 2, 4 and 6 wt.-% of nano-$Al_2O_3$ incorporated Al composites, while relative-

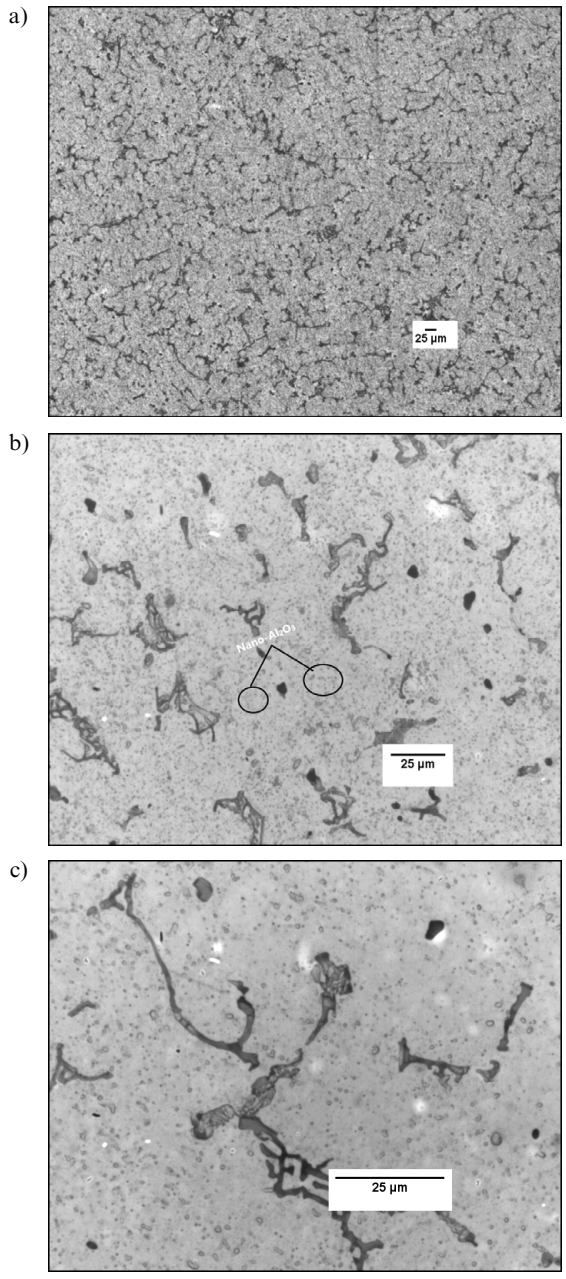


**Figure 1.** Al 5083 alloy reinforced with, 2% Nano $Al_2O_3$ (a) 100X (b) 500X (c) 1000X.

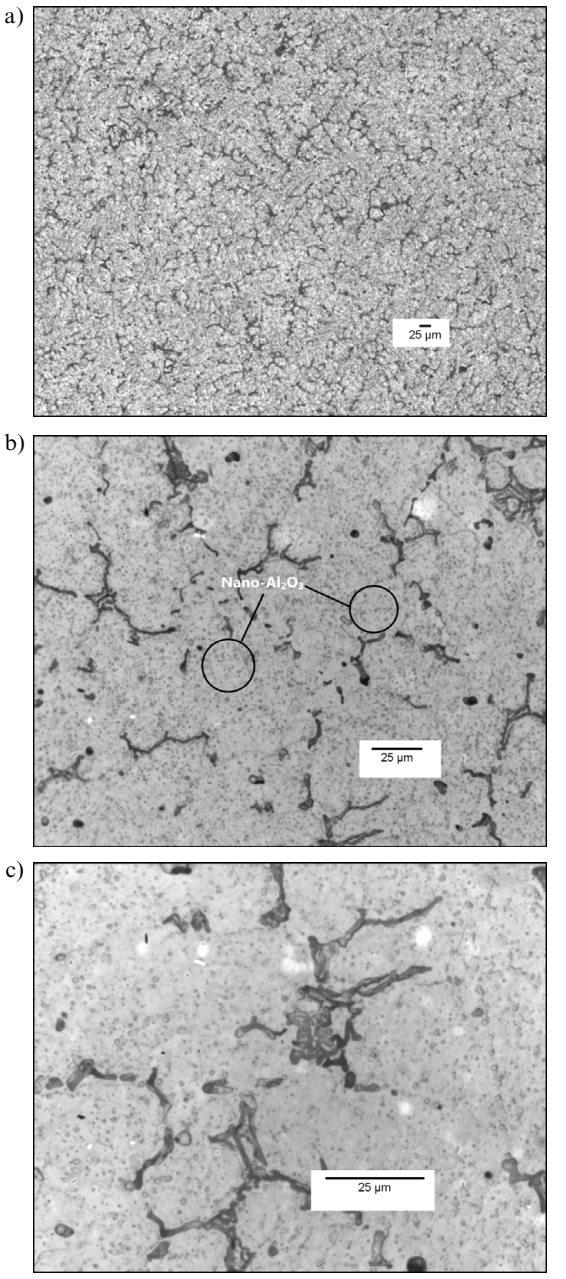


**Figure 2**. Al 5083 alloy reinforced with, 4% Nano $Al_2O_3$ (a) 100X (b) 500X (c) 1000X.

ly notable amount of agglomeration was observed in 8% nano-$Al_2O_3$ incorporated Al MMCs (Fig. 5). Microstructure images depict fine precipitates of nano-$Al_2O_3$ dispersed along grain boundary in the Al matrix. Thus, nearly homogeneous dispersion of nano-particles was attained. The Micro-hardness test was carried out on the Brinell hardness tester as per ASTM E10 (2018) at a load of 31.25 kgf. The average of 5 trials was considered to determine the hardness value of each specimen and results are illustrated in Table 3. There was an increase in hardness with an increased percentage of $Al_2O_3$ till 6 wt.-% and decreased marginally for 8 wt.-%. The hard $Al_2O_3$ particles perhaps caused a barrier for initial stresses. Besides, nearly uniform dispersion of $Al_2O_3$ particles in the matrix has decreased the inter-spatial gap, resulting in pile-up of dislocations. The work hardening of the matrix alloy increases due to $Al_2O_3$ reinforcement thereby increasing the load required for the nucleation and propagation of voids. Hence, an increase in hardness was observed. In addition, increase in hardness owes to Hall-Petch hardening effect (Jenczyk *et al.*, 2021). Further increase in $Al_2O_3$ caused a marginal decrease in hardness. It may be because an in-

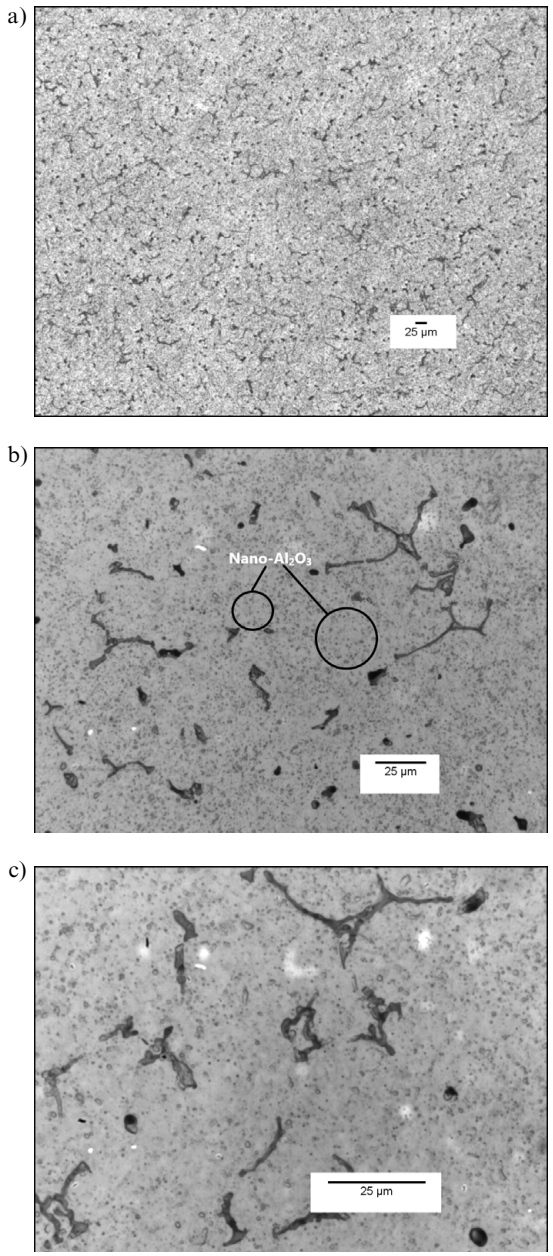


**Figure 3**. Al 5083 alloy reinforced with, 6% Nano $Al_2O_3$ (a) 100X (b) 500X (c) 1000X.

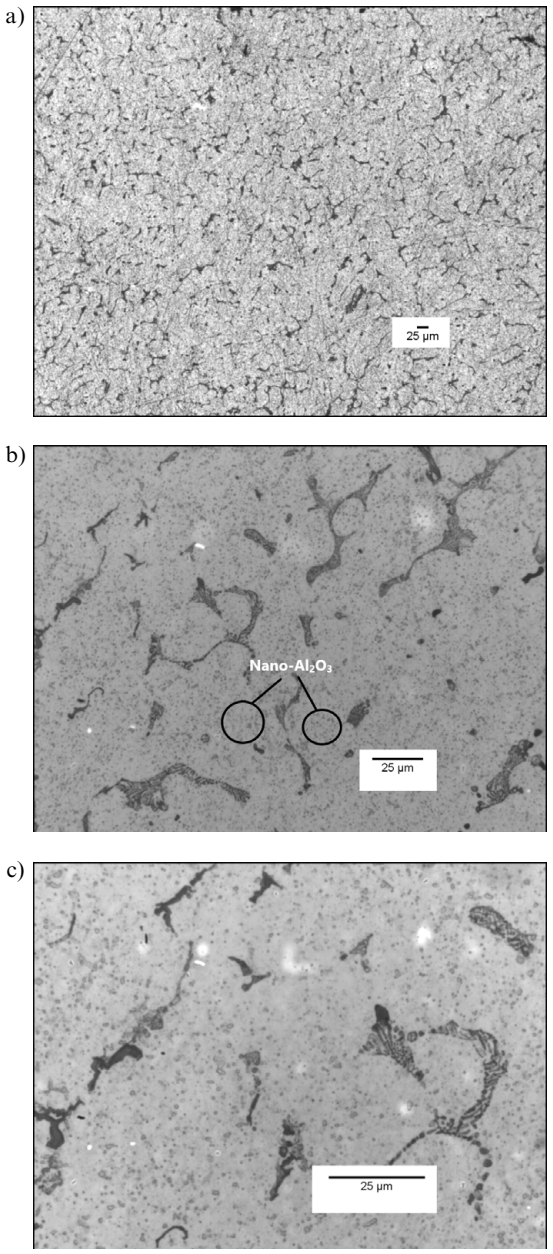


**Figure 4.** Al 5083 alloy reinforced with, 8% Nano $Al_2O_3$ (a) 100X (b) 500X (c) 1000X.

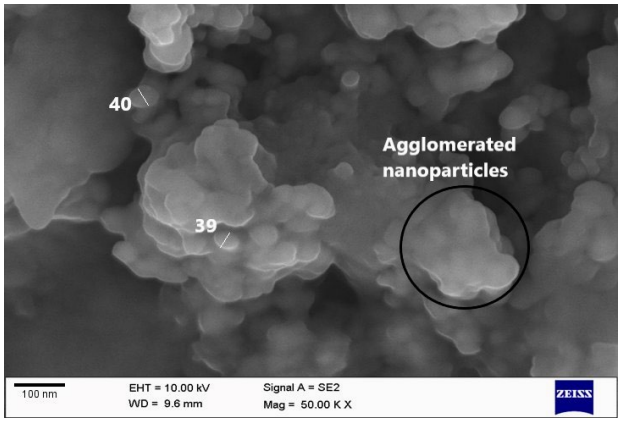


**Figure 5.** High magnification SEM image of 8% Nano $Al_2O_3$/Al MMC illustrating agglomeration

**Table 4:** Elemental composition of Al 5083 alloy reinforced with, 6% Nano $Al_2O_3$

| Element | APP Conc. | Intensity Corrn. | Weight % |
|---|---|---|---|
| Mn K | 4.01 | 0.1681 | 4.68 |
| Al K | 132.01 | 1.1881 | 70.25 |
| O K | 8.33 | 0.6374 | 8.19 |
| Mg K | 7.23 | 0.974 | 12.35 |
| Si K | 4.82 | 0.5048 | 2.88 |
| Fe k | 3.5 | 0.8519 | 2.57 |
| Total | | | 100.00 |

crease in nano-particles leads to increased particle to particle affinity and greater surface to volume ratio. It has caused the agglomeration of particles, resulting in uneven dispersion of reinforcement in the matrix. Similar observations were made in available research

**Table 3:** Hardness of the studied specimens

| Sl. No. | Composition | Brinell Hardness (BHN) |
|---|---|---|
| 1 | AA5083 | 58.6±0.7 |
| 2 | AA5083+2wt.-% $Al_2O_3$ | 60.2±1.2 |
| 3 | AA5083+4wt.-% $Al_2O_3$ | 62.5±1.1 |
| 4 | AA5083+6wt.-% $Al_2O_3$ | 63.8±0.8 |
| 5 | AA5083+8wt.-% $Al_2O_3$ | 63.3±1.0 |

(Ma *et al.*, 2017). Figure 6 shows the EDS spectrum of Al 5083 alloy reinforced with, 6% nano-$Al_2O_3$, from the figure it was evident that Al and O are present, which confirms the presence of nano-$Al_2O_3$ in the Al5083 matrix. Also, the weight percentage of each element in the composition is shown in Table 4.

## 2.4. Design of experiments

Taguchi-based experimental design has been employed to acquire experimental data systematically. Taguchi's L25 orthogonal array was chosen for investigation since it allows operating three parameters each at five levels (Table 5). The obtained results were analyzed using Analysis of Variance (ANOVA) to study the significance of each parameter. The response studied was wear, whose experimental average was computed for three repetitions to achieve the minimum experimental error. ANOVA was carried out for one response and three variables using smaller the better quality characteristic since the objective of the investigation was to minimize wear. MINITAB-17®, a statistical package was used to

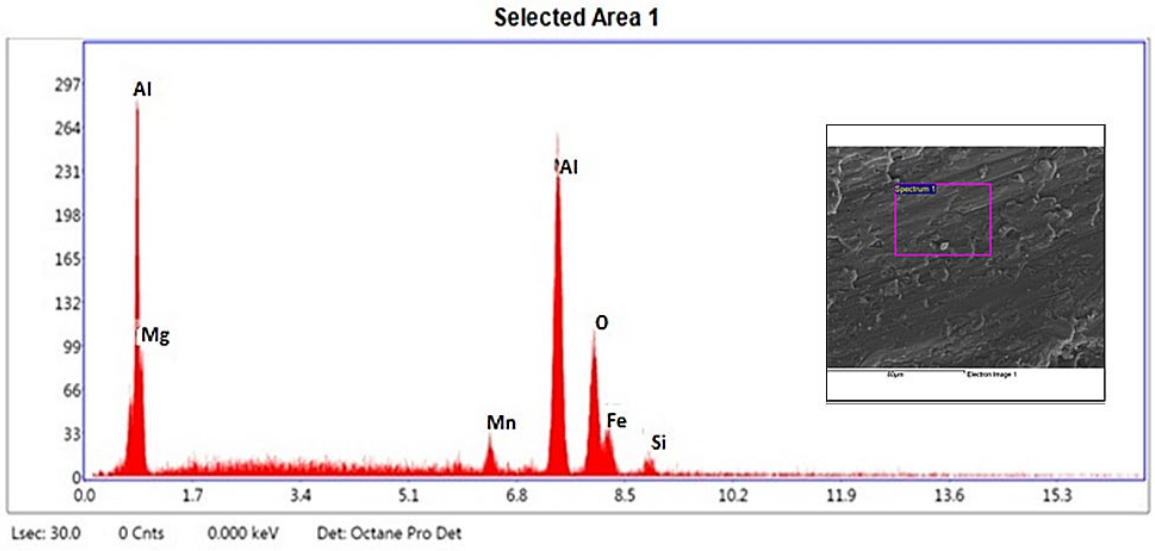


**Figure 6.** EDS Spectrum of Al 5083 alloy reinforced with, 6% Nano $Al_2O_3$.

**Table 5:** L25 Orthogonal array and experimental results of Wear

| Trial No. | % reinforcement | Load (N) | Sliding Distance (m) | Wear (μm) | Specific Wear Rate ($\times 10^{-3}$ $mm^3$/N-m) |
|---|---|---|---|---|---|
| **1** | 0 | 4.905 | 1000 | 41 ±1 | 1.530 |
| **2** | 0 | 9.81 | 2000 | 105±7 | 1.076 |
| **3** | 0 | 14.715 | 3000 | 187±12 | 0.852 |
| **4** | 0 | 19.62 | 4000 | 312±17 | 0.799 |
| **5** | 0 | 24.525 | 5000 | 421±24 | 0.690 |
| **6** | 2 | 4.905 | 2000 | 74±7 | 1.517 |
| **7** | 2 | 9.81 | 3000 | 136±14 | 0.929 |
| **8** | 2 | 14.715 | 4000 | 221±11 | 0.755 |
| **9** | 2 | 19.62 | 5000 | 344±23 | 0.705 |
| **10** | 2 | 24.525 | 1000 | 67±5 | 0.549 |
| **11** | 4 | 4.905 | 3000 | 92±5 | 1.300 |
| **12** | 4 | 9.81 | 4000 | 160±7 | 0.820 |
| **13** | 4 | 14.715 | 5000 | 247±12 | 0.675 |
| **14** | 4 | 19.62 | 1000 | 51±3 | 0.523 |
| **15** | 4 | 24.525 | 2000 | 133±6 | 0.545 |
| **16** | 6 | 4.905 | 4000 | 102±4 | 1.150 |
| **17** | 6 | 9.81 | 5000 | 156±8 | 0.640 |
| **18** | 6 | 14.715 | 1000 | 35±1 | 0.478 |
| **19** | 6 | 19.62 | 2000 | 98±4 | 0.502 |
| **20** | 6 | 24.525 | 3000 | 180±13 | 0.480 |
| **21** | 8 | 4.905 | 5000 | 149±11 | 1.210 |
| **22** | 8 | 9.81 | 1000 | 28±1 | 0.570 |
| **23** | 8 | 14.715 | 2000 | 86±2 | 0.588 |
| **24** | 8 | 19.62 | 3000 | 157±7 | 0.540 |
| **25** | 8 | 24.525 | 4000 | 262±13 | 0.520 |

perform statistical analysis. The linear regression model was developed to correlate studied parameters with wear. Subsequently, the presented model helps to predict wear within the studied range of parameters. The main effect plots and rank analysis were employed to analyze the influence of each parameter on the response.

## 3. RESULTS AND DISCUSSION

### 3.1. Effect of parameters on wear

Table 5 illustrates results obtained for various combinations of parameter levels as per the L25 orthogonal array for wear and specific wear rate. ANOVA was used to find out the effect of each input parameter on wear characteristics of prepared nanocomposites. It aids to determine significant parameters and percentage contributions of the individual parameter on wear behavior. The analysis of performance criteria based on ANOVA during wear test and percentage contribution of parameters were evaluated for a significance level of 0.05 or

**Table 6:** ANOVA analysis for wear

| Source | DOF | Adj SS | Adj MS | F-Value | P-Value | Remarks | % Contribution |
|---|---|---|---|---|---|---|---|
| **Sliding Distance** | 4 | 111497 | 27874.25 | 16.294 | 0.000 | Significant | 55.42 |
| **Load** | 4 | 56677 | 14169.25 | 8.282 | 0.000 | Significant | 27.77 |
| **% of reinforcement** | 4 | 25307 | 6326.75 | 3.698 | 0.000 | Significant | 11.95 |
| **Error** | 12 | 4815 | 401.25 | | | | 4.86 |
| **Total** | 24 | 198296 | | | | | 100 |

**Table 7:** ANOVA analysis for the specific wear rate

| Source | DOF | Adj SS | Adj MS | F-Value | P-Value | Remarks | % Contribution |
|---|---|---|---|---|---|---|---|
| **% of reinforcement** | 4 | 0.40282 | 0.100706 | 39.48 | 0.000 | Significant | 55.42 |
| **Load** | 4 | 2.01904 | 0.504759 | 197.88 | 0.000 | Significant | 27.77 |
| **Sliding Distance** | 4 | 0.03844 | 0.009611 | 3.77 | 0.033 | Significant | 11.95 |
| **Error** | 12 | 0.03061 | 0.002551 | | | | 4.86 |
| **Total** | 24 | 2.49092 | | | | | 100 |

confidence interval of 95%. It implies that a source having less than 0.05 P value was considered a statistically significant parameter. ANOVA results for wear and specific wear rate are shown in Table 6 and 7 respectively. It was observed that the P-value for all sources was less than 0.05 suggesting the statistical significance of each studied parameter.

ANOVA analysis and rank analysis (Table 8 and 9) suggests that the sliding distance was the highest influencing factor on wear followed by the applied load. The percentage of reinforcement was the least influencing factor. On contrary, the applied load and percentage of reinforcement was the most significant factor. While, sliding distance was the least significant influencing factor on the specific wear rate. Besides, it can be observed that the studied parameters were statistically significant factors and affects the wear rate of developed composites. According to the main effect plot for means, the least value of the mean of means for the respective parameter will result in a minimum rate of wear which was the objective of the study. Figure 6b and Fig. 7a illustrates the main effect plot for wear and specific wear rate. Wear loss was found to increase with the increase in the reinforcement percentage, while a decrease in specific wear rate has observed. It was observed that wear is minimum at level 4% of reinforcement i.e. 6 wt.-%, while at level 1 for Load and sliding distance i.e., 4.905 N and 1000 m respectively. The higher hardness was obtained for the 6% reinforced MMC. The higher hardness corresponds

**Table 8:** Response Table for Means for the Wear

| **Level** | **% reinforcement** | **Load** | **Sliding Distance** |
|---|---|---|---|
| 1 | 213.2 | 91.60 | 44.40 |
| 2 | 168.4 | 117.00 | 99.20 |
| 3 | 136.6 | 155.20 | 150.40 |
| 4 | 114.2 | 192.40 | 211.40 |
| 5 | 136.4 | 212.60 | 263.40 |
| Delta | 99.40 | 121.00 | 219.00 |
| Rank | 3 | 2 | 1 |

**Table 9:** Response Table for Means for the Specific Wear Rate

| Level | % Reinforcement | Load | **Sliding Distance** |
|---|---|---|---|
| 1 | 0.449 | -2.4923 | 3.6865 |
| 2 | 1.5393 | 2.0979 | 2.3224 |
| 3 | 2.7523 | 3.6542 | 2.2958 |
| 4 | 4.2864 | 4.3896 | 2.1151 |
| 5 | 3.7754 | 5.1489 | 2.3785 |
| Delta | 3.8416 | 7.6411 | 1.5714 |
| Rank | 2 | 1 | 3 |

to the higher wear resistance of the composite sample with additions of $Al_2O_3$ reinforcement (Siddesh Kumar *et al.*, 2016). Thus, the minimum wear was

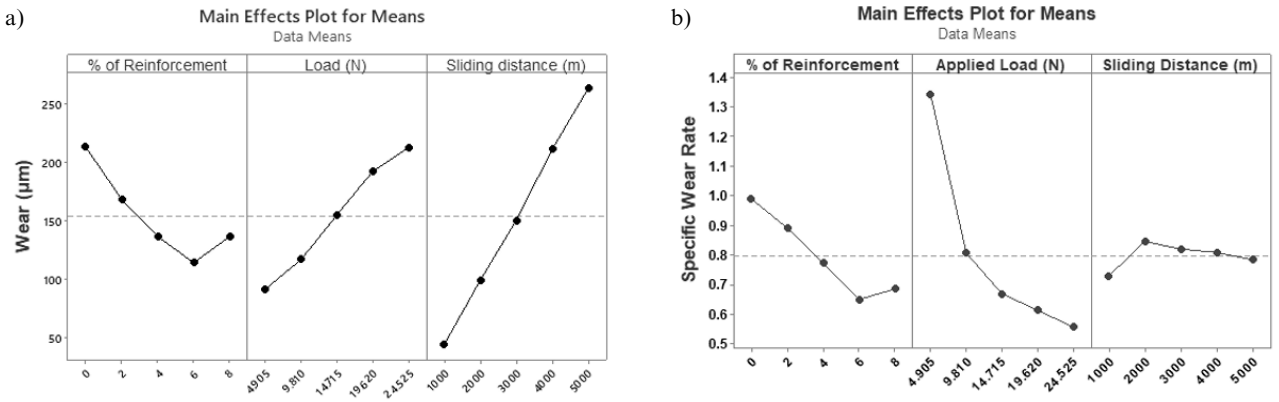


**Figure 7.** (a) Main effect plot of factors affecting the wear, and (b) Main effect plot of factors affecting specific wear rate.

obtained for the Al/6%-nano$Al_2O_3$ composite specimen. The values of wear increased with an increase in the applied load and wear rate was found to decrease with the increase in load. The reinforcement possesses the ability to withstand an applied load to a certain level within which wear is attributed only to mild wear. At a higher level of load, the transition of mild to severe wear has occurred. Perhaps, a higher load resulted in an increased of the high surface stresses and led to severe material loss. The wear of the specimen was increased with an increase in the sliding distance significantly. The wear rises sharply above 2000 m due to increased interaction between counterparts. During the initial condition, the matrix with strongly bonded particles is in contact with a hard rotating disc resisting the wear loss. In the later stage, particles were removed along with the matrix resulting in increased of the wear loss. Thus, severe wear was observed at higher levels of sliding distance. While, sliding distance has increase specific wear rate initially owing to matrix removal. The further increase in sliding distance has resulted in decrease of specific wear rate perhaps revealing the exposure of reinforcement particles.

### 3.2. Regression model

The obtained results were fitted as a linear regression model, which aids to correlate wear with studied parameters viz. percentage of reinforcement, applied load and sliding distance. The model was developed using Minitab® 17 statistical package and is presented as Eq. (1).

$$W=-65-(10.39\times P)+(6.471\times L)+(0.05502\times D) \quad (1)$$
R-Sq.: 91.58%; R-Sq.(Adj):90.38%;

where P is the percentage of reinforcement of nano-$Al_2O_3$, L is the applied load and D is the sliding distance. The feasibility of any developed models can be understood and studied through $R^2$ and $R^2$ (adj) and validation is attained with the help of confirmation tests. The $R^2$ and $R^2$ (adj) values obtained for developed equations are 91.58% and 90.38%. Thus, the presented equation is adequate and feasible to predict wear within the studied range of parameters. Further, to validate the model, confirmation tests were conducted at the random value of parameters within the studied range viz. the sliding distance of 4500 m and 19.62 N applied load for the alloy and the different MMC specimens as shown in Table 10. The experimental and regression equation predicted values of wear were compared and corresponding error percentage values are illustrated. The computed percentage error for wear was less than 10%. Thus, it can be concluded that the presented wear model is adequate and can be successfully used to predict wear satisfactorily.

### 3.3. Worn surface morphology

Figure 8 (a-e) shows SEM images of worn surfaces for various materials studied at 4500 m and 19.62 N of sliding distance and load, respectively. The wear behavior of MMCs reinforced with nano-$Al_2O_3$ particles has been investigated in the present study. The

**Table 10:** Results of the confirmation test

| Trial Nº | % Reinforcement | Load (N) | Sliding distance (m) | Exp. Wear (µm) | Predicted Wear (µm) | % Error |
|---|---|---|---|---|---|---|
| 1 | 0 | 19.62 | 4500 | 331±2 | 310 | 6.48 |
| 2 | 2 | 19.62 | 4500 | 274±12 | 289 | 5.39 |
| 3 | 4 | 19.62 | 4500 | 249±9 | 268 | 7.63 |
| 4 | 6 | 19.62 | 4500 | 225±14 | 247 | 9.87 |
| 5 | 8 | 19.62 | 4500 | 237±17 | 226 | 4.46 |

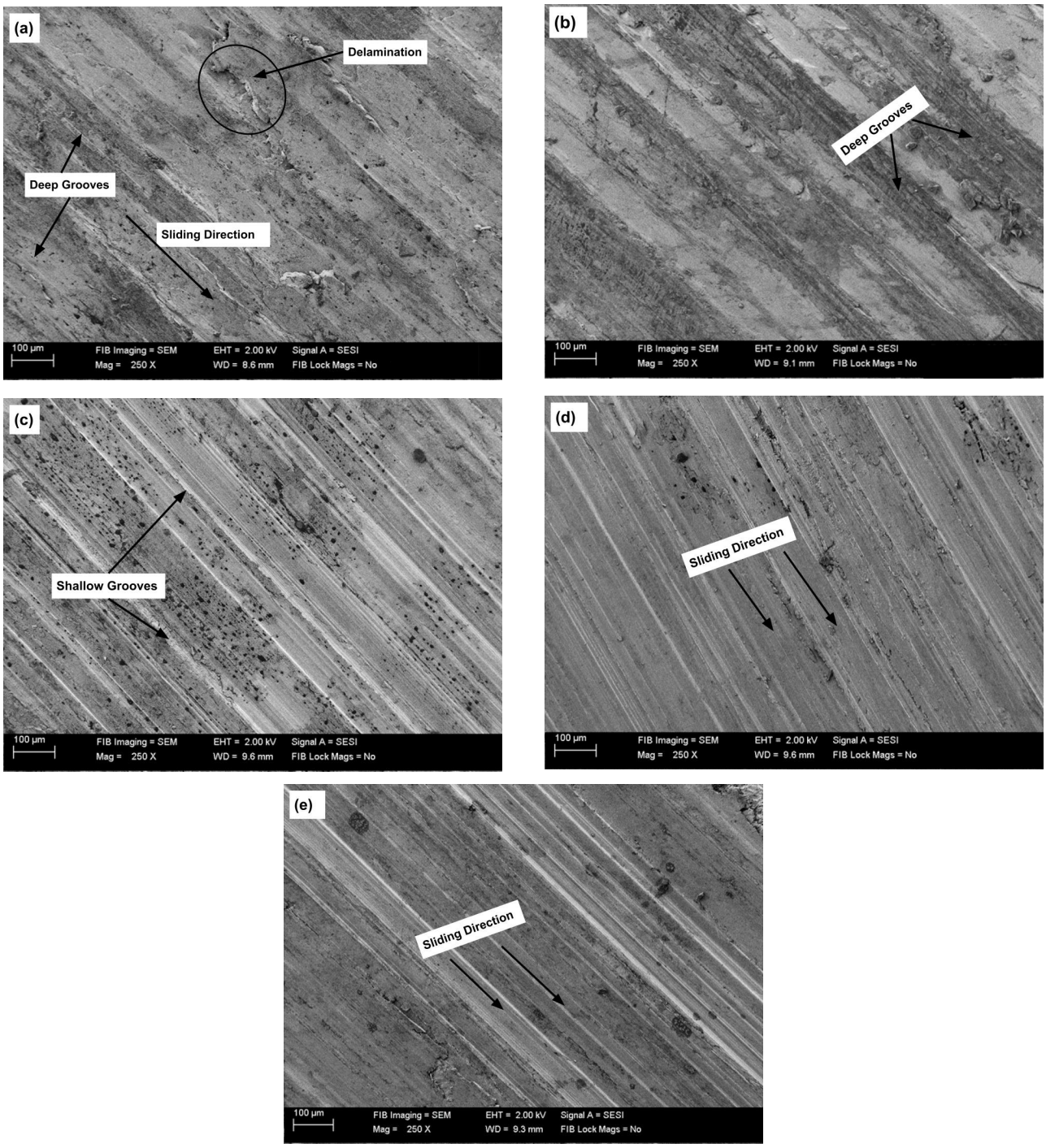


**Figure 8.** SEM image of worn surface at 4500 m and 19.62 N sliding distance and load respectively for (a) AA 5083 alloy, (b) AA 5083 + 2% of $Al_2O_3$, (c) AA 5083 + 4% of $Al_2O_3$, (d) AA 5083 + 6% of $Al_2O_3$, (e) AA 5083 + 8% of $Al_2O_3$.

analysis has revealed that an increase in the load and the sliding distance has increased wear. At low load conditions, sliding wear occurs with minimum loss due to low contact stress. While, the increase in load is attributed to an increase in contact stress, which leads to the rapid growth of wear. In addition, increased high load condition results in an increase of the temperature at the pin-disc interface, perhaps due to the induced large contact stress and friction. It causes delamination of the surface layer and transfer of pin material to counterface occurs (Basavarajappa *et al.*, 2007). Hence, the transition of mild to severe wear was observed with variation of the load from a low to a high value during the study.

The wear was increased drastically with an increase in the sliding distance. During the initial stages, the surface layer of the pin was in contact with the counter-face. The irregularities existing on the pin surface undergo plastic deformation and detach progressively from its parent metal. It results in the formation of a protective mechanical mixed layer between two counterparts. Further, hard reinforcement particles present in tested MMCs resist deformation and arrest dislocation movement. While an increase in the sliding distance increases the interaction between counterparts and the applied load has further supported for disruption of the protective layer. Besides, incorporated particles in the MMCs come out of pins due to wear and were entrapped between counterparts. The hard asperities have caused the transformation of sliding wear into three-body abrasive wear. Thus, grooves were observed in a sliding direction on worn surface images (Fig. 8). Hence, greater wear of the specimen was observed at higher sliding distance conditions. The obtained results agree with the Archard model, which states that wear is directly proportional to the load and the sliding distance (Archard, 1953).

The results obtained indicated that there exists a threshold value beyond which the percentage of reinforcement leads to a deterioration of the tribological property. The particulate incorporation into Al alloy has enhanced its wear resistance. It may be due to the fact that, particulate incorporated MMCs possess high surface energy and acts as a barrier for the penetration of wear debris during sliding phenomenon. Further, burrs formed due to the plowing of counter surface asperities get detached from the worn surface. The detached debris of worn surface exists as loose debris between pin-disc interface. Also, they possess a hard and abrasive nature. The debris acts as a plowing agent under contact force and accelerates wear.

The SEM image for the worn surface of AA5083 is shown in Fig. 8a. Deep and wider grooves are present in the direction of sliding. It could well correspond to the characteristics of severe abrasive wear due to hard asperities or wear debris between surfaces in contact (Yao *et al.*, 2015). Plastic flow during abrasion generates high shear stresses on the surface. Subsequently, frictional heat gives rise to delamination wear, thus increasing the depth of the groove (Joshua *et al.*, 2018). In addition, the resistance offered against the wear debris penetration was relatively inadequate in the neat alloy. Hence, deterioration of the surface was observed in a larger area. Fig. 8b shows the worn surface of AA5083+2wt.-%$Al_2O_3$. Deep grooves persist which can be attributed to abrasive wear. Besides, the incorporation of nanoparticles means a relatively enhanced surface barrier for the penetration of worn-out particles. Subsequently, combined wear mechanisms of plastic deformation and progressive removal of embedded particles has occurred, resulting in wear.

Figure 8 (c-d) correspond to AA5083+4wt.-%$Al_2O_3$ and AA5083+6wt.-%$Al_2O_3$ worn surface images. They reveal the presence of shallow grooves, indicating the occurrence of abrasive wear, because of micro plowing and cutting, while plastic deformation was least observed. It may be because an increase in the reinforcement percentage has resulted in an increased in hardness. Subsequently, surface energy required for the detachment of the surface layer has increased drastically (Shivakumar *et al.*, 2015). Thus, sliding wear resistance has enhanced; yet, the entrapped hard asperities of worn debris present between counterparts has caused abrasive wear. Hence, the dominant wear mechanism observed for 4% and 6% nanoparticles reinforced MMCs was a three-body abrasive wear mechanism, instead of sliding wear. Besides, the dark spots in Fig. 8c indicate the occurrence of oxidation of the tested specimen. Further, it suggests the dominant phenomenon of oxidative wear mechanism in 4% $Al_2O_3$ incorporated MMC.

Figure 8e shows the worn surface of AA5083+8wt.-%$Al_2O_3$. Similar wear pattern comprising thin grooves can be seen on the surface with slightly wider grooves for 8 wt.-%. The high content of nano-$Al_2O_3$ and high dislocation density of deformed planes results in mild abrasion, thereby reducing the loss of material (Kumar and Rajadurai, 2016). Further, having a higher reinforcement percentage resulted in poor boding strength and poor resistance to plastic deformation due to the decrement of hardness. Therefore, a higher number of worn-out lose particles was observed compared to 6% nanoparticles reinforced MMC. Further, a small amount of metal fold indicates plastic deformation and grooves, suggesting abrasive wear is present on the work surface. Hence, both types of wear mechanisms were observed in the 8% nanoparticles reinforced MMC. However, abrasive wear was dominant due to a large number of entrapped worn-out particles between contact surfaces.

## 4. CONCLUSIONS

The conclusions are drawn from the microstructure study, hardness and dry sliding wear experimentation of AA5083/nano-$Al_2O_3$ MMCs were as follows.

- The microstructure analysis of prepared composites ensures nearly uniform dispersion of reinforcement within matrix.
- The study indicated that hardness was superior for MMCs compared to the unreinforced alloy. However, hardness was increased to 6% reinforcement, but further increase in the re-

inforcement percentage resulted in a drop of hardness.

- The main effect plots illustrated an increase of wear, as the applied load and the sliding distance increases. Besides, wear decreased with an increase in the percentage of reinforcement till 6% reinforcement; further increment of the particle reinforcement percentage lead to a deterioration of wear resistance attributed to a variation of hardness.
- ANOVA results revealed that the sliding distance was the highest significant parameter on wear followed by the load and the reinforcement percentage. It was further ensured through response rank analysis.
- The linear regression model has been presented to correlate the studied parameters with wear. The $R^2$ and $R^2$(adj) values of the model are greater than 90%, confirming the adequacy of the model. In addition, the feasibility of models was ensured through confirmation tests. The results from the experiments and the model predictions were compared. The error percentage was well within an acceptable range (<10%).
- The worn surface morphology depicted that, plastic deformation was the predominant wear mechanism for AA5083, while abrasive wear was predominant in particle reinforced MMCs. Furthermore, the deterioration of the surface was relatively lower in the nano-$Al_2O_3$ reinforced MMCs compared to neat alloy, revealing superior wear resistance.

## REFERENCES


Archard, J.F. (1953). Contact and Rubbing of Flat Surfaces. *J. Appl. Phys.* 24, 981-988. https://doi.org/10.1063/1.1721448.

ASTM G99 (2017). Standard Test Method for Wear Testing with a Pin-on-Disk Apparatus. ASTM International, West Conshohocken, PA, USA.

ASTM E10 (2018). Standard Test Method for Brinell Hardness of Metallic Materials. ASTM International, West Conshohocken, PA, USA.

Azimi, A., Shokuhfar, A., Nejadseyfi, O., Fallahdoost, H., Salehi, S. (2015). Optimizing consolidation behavior of Al 7068-TiC nanocomposites using Taguchi statistical analysis. *Trans. Nonferrous Met. Soc. China* 25 (8), 2499–2508. https://doi.org/10.1016/S1003-6326(15)63868-7.

Basavarajappa, S., Chandramohan, G., Paulo Davim, J. (2007). Application of Taguchi techniques to study dry sliding wear behaviour of metal matrix composites. *Mater. Design* 28 (4), 1393–1398. https://doi.org/10.1016/j.matdes.2006.01.006.

Casati, R., Vedani, M. (2014). Metal matrix composites reinforced by Nano-Particles—A review. *Metals* 4 (1), 65–83. https://doi.org/10.3390/met4010065.

Cavdar, U., Gezici, L.U., Gul, B., Avyaz, M., (2020). Microstructural properties and tribological behaviours of Ultra-High frequency induction rapid sintered Al-WC composites. *Rev. Metal.* 56 (1), e163. https://doi.org/10.3989/revmetalm.163.

Çömez, N. (2021) Wear behavior and corrosion properties of Age-hardened AA2010 aluminum alloy. *Rev. Metal.* 57 (3), e201. https://doi.org/10.3989/revmetalm.201.

Ekka, K.K., Chauhan, S.R., Varun (2014). Dry Sliding Wear Characteristics of SiC and $Al_2O_3$ Nanoparticulate Aluminium Matrix Composite Using Taguchi Technique. *Arab. J. Sci. Eng.* 40 (2), 571–581. https://doi.org/10.1007/s13369-014-1528-2.

Ekka, K.K., Chauhan, S.R., Varun (2015). Dry Sliding Wear Characteristics of SiC and $Al_2O_3$ Nanoparticulate Aluminium Matrix Composite Using Taguchi Technique. *Arab. J. Sci. Eng.* 40, 571–581. https://doi.org/10.1007/s13369-014-1528-2.

El-Kady, E.-S., Khalil, T., Tawfeek, T. (2015). Experimental Investigations towards Optimization of the Parameters for Wear Loss Quantities in A356/$Al_2O_3$ Nanocomposites. *Am. J. Mater. Eng. Technol.* 3 (1), 1–6. https://doi.org/10.12691/materials-3-1-1.

Essa, F.A., Elsheikh, A.H., Yu, J., Elkady, O.A., Saleh, B. (2021). Studies on the effect of applied load, sliding speed and temperature on the wear behavior of M50 steel reinforced with $Al_2O_3$ and / or graphene nanoparticles. *J. Mater. Res. Technol.* 12, 283-303. https://doi.org/10.1016/j.jmrt.2021.02.082.

Ezatpour, H.R., Sajjadi, S.A., Sabzevar, M.H., Huang, Y. (2014). Investigation of microstructure and mechanical properties of Al6061-nanocomposite fabricated by stir casting. *Mater. Design* 55, 921–928. https://doi.org/10.1016/j.matdes.2013.10.060.

Ezatpour, H.R., Torabi Parizi, M., Sajjadi, S.A., Ebrahimi, G.R., Chaichi, A. (2016). Microstructure, mechanical analysis and optimal selection of 7075 aluminum alloy based composite reinforced with alumina nanoparticles. *Mater. Chem. Phys.* 178, 119–127. https://doi.org/10.1016/j.matchemphys.2016.04.078.

Gargatte, S., Upadhye, R.R., Dandagi, V.S., Desai, S.R., Waghamode, B.S. (2013). Preparation & Characterization of Al-5083 Alloy Composites. *JMMCE* 1 (1), 8–14. https://doi.org/10.4236/jmmce.2013.11002.

Idrisi, A.H., Mourad, A.H.I., Thekkuden, D.T., Christy, J.V. (2018). Wear behavior of AA 5083/SiC nano-particle metal matrix composite: Statistical analysis. *IOP Conf. Ser.: Mater. Sci. Eng.* 324, 012087. https://doi.org/10.1088/1757-899X/324/1/012087.

Jenczyk, P., Grzywacz, H., Milczarek, M., Jarzabek, D.M. (2021) Mechanical and Tribological Properties of Co-Electrodeposited Particulate-Reinforced Metal Matrix Composites: A Critical Review with Interfacial Aspects. *Materials* 14 (12), 3181. https://doi.org/10.3390/ma14123181.

Jeyasimman, D., Sivasankaran, S., Sivaprasad, K., Narayanasamy, R., Kambali, R.S. (2014). An investigation of the synthesis, consolidation and mechanical behaviour of Al 6061 nanocomposites reinforced by TiC via mechanical alloying. *Mater. Design* 57, 394–404. https://doi.org/10.1016/j.matdes.2013.12.067.

Joshua, K.J., Vijay, S.J., Selvaraj, D.P. (2018). Effect of nano $TiO_2$ particles on microhardness and microstructural behavior of AA7068 metal matrix composites. *Ceram. Int.* 44 (17), 20774–20781. https://doi.org/10.1016/j.ceramint.2018.08.077.

Kim, K.T., Cha, S. Il, Hong, S.H. (2007). Hardness and wear resistance of carbon nanotube reinforced Cu matrix nanocomposites. *Mater. Sci. Eng.* A 449–451, 46–50. https://doi.org/10.1016/j.msea.2006.02.310.

Kok, M. (2005). Production and mechanical properties of $Al_2O_3$ particle-reinforced 2024 aluminium alloy composites. J. Mater. *Process. Technol.* 161 (3), 381–387. https://doi.org/10.1016/j.jmatprotec.2004.07.068.

Kumar, H., Chaudhari, G.P. (2014). Creep behavior of AS41 alloy matrix nano-composites. *Mater. Sci. Eng.* A 607, 435–444. https://doi.org/10.1016/j.msea.2014.04.020.

Kumar, C.A.V., Rajadurai, J.S. (2016). Influence of rutile ($TiO_2$) content on wear and microhardness characteristics of aluminium-based hybrid composites synthesized by powder metallurgy. *Trans. Nonferrous Met. Soc. China* 26 (1), 63–73. https://doi.org/10.1016/S1003-6326(16)64089-X.

Kumar, R.A., Devaraju, A., Arunkumar, S. (2018). Experimental Investigation on Mechanical Behaviour and Wear

Parameters of TiC and Graphite Reinforced Aluminium Hybrid Composites. *Mater. Today-Proc.* 5 (6), 14244–14251. https://doi.org/10.1016/j.matpr.2018.03.005.

Ma, P., Jia, Y., Gokuldoss, P. konda, Yu, Z., Yang, S., Zhao, J., Li, C. (2017). Effect of $Al_2O_3$ nanoparticles as reinforcement on the tensile behavior of Al-12Si composites. *Metals* 7 (9), 359. https://doi.org/10.3390/met7090359.

Mobasherpour, I., Tofigh, A.A., Ebrahimi, M. (2013). Effect of nano-size $Al_2O_3$ reinforcement on the mechanical behavior of synthesis 7075 aluminum alloy composites by mechanical alloying. *Mater. Chem. Phys.* 138 (2–3), 535–541. https://doi.org/10.1016/j.matchemphys.2012.12.015.

Mousavian, R.T., Behnamfard, S., Heidarzadeh, A., Taherkhani, K., Khosroshahi, R.A., Brabazon, D. (2021) Incorporation of SiC Ceramic Nanoparticles into the Aluminum Matrix by a Novel Method: Production of a Metal Matrix Composite. *Met. Mater. Int.* 27, 2968–2976. https://doi.org/10.1007/s12540-019-00604-9.

Moustafa, E., Khalil, A., Haitham, A., Hefni, M., Mosleh, A.O. (2021). Microstructure, Hardness, and Wear Behavior Investigation of the Surface Nanocomposite Metal Matrix Reinforced by Silicon Carbide and Alumina Nanoparticles. *J. Miner. Metal Mater.* Eng. 7, 57-62.

Narasimha Murthy, I., Venkata Rao, D., Babu Rao, J. (2012). Microstructure and mechanical properties of aluminum-fly ash nano composites made by ultrasonic method. *Mater. Design* 35, 55–65. https://doi.org/10.1016/j.matdes.2011.10.019.

Padhi, P., Kar, S. (2011). A novel route for development of bulk Al/SiC metal matrix nanocomposites. *J. Nanotechnol.* ID 413512. https://doi.org/10.1155/2011/413512.

Pang, X., Xian, Y., Wang, W., Zhang, P. (2018). Tensile properties and strengthening effects of 6061Al/12wt.%B4C composites reinforced with nano-$Al_2O_3$ particles. *J. Alloys Compd.* 768, 476–484. https://doi.org/10.1016/j.jallcom.2018.07.072.

Raturi, A., Mer, K.K.S., Kumar Pant, P. (2017). Synthesis and characterization of mechanical, tribological and micro structural behaviour of Al 7075 matrix reinforced with nano $Al_2O_3$ particles. *Mater. Today-Proc.* 4 (2), 2645–2658. https://doi.org/10.1016/j.matpr.2017.02.139.

Ray, V.K., Padhi, P., Jha, B.B., Sahoo, T.K. (2015). Wear characteristics of pure aluminium, al-alloy & al-alumina metal mtrix nano composite in dry condition: Part-I. *IJRET* 4 (7), 17–25.

Shivakumar, N., Vasu, V., Narasaiah, N., Kumar, S. (2015). Synthesis and Characterization of Nano-sized $Al_2O_3$ Particle Reinforced ZA-27 Metal Matrix Composites. *Procedia Materials Science* 10, 159–167. https://doi.org/10.1016/j.mspro.2015.06.037.

Siddesh Kumar, N.G., Ram Prabhu, T., Shiva Shankar, G.S., Basavarajappa, S. (2016). Dry sliding wear properties of unhybrid and hybrid Al alloy based nanocomposites. *Tribol. – Mater. Surf. Interfaces* 10 (3), 138–149. https://doi.org/10.1080/17515831.2016.1247132.

Singh, R.K., Kumar, D., Kumar, A. (2015). Wear Behavior of Al-SiC-Cu Metal Matrix Composites Prepared by Stir Casting and Optimization by using Taguchi Method. *J. Material Sci. Eng.* 4 (5), 1–4. https://doi.org/10.4172/2169-0022.1000185.

Somani N., Gupta N.K., (2021). Effect of TiC nanoparticles on microstructural and tribological properties of Cu-TiC nano-composites. *Proc. Inst. Mech. Eng. B: J. Eng. Manuf.* 236 (4), 319-336. https://doi.org/10.1177/09544054211029828.

Srivyas, P.D., Charoo, M.S. (2018). Role of Fabrication Route on the Mechanical and Tribological Behavior of Aluminum Metal Matrix Composites - A Review. *Mater. Today-Proc.* 5 (9), 20054–20069. https://doi.org/10.1016/j.matpr.2018.06.372.

Tu, J.P., Rong, W., Guo, S.Y., Yang, Y.Z. (2003). Dry sliding wear behavior of in situ Cu-$TiB_2$ nanocomposites against medium carbon steel. *Wear* 255 (7–12), 832–835. https://doi.org/10.1016/S0043-1648(03)00115-7.

Yao, Y.T., Jiang, L., Fu, G.F., Chen, L.Q. (2015). Wear behavior and mechanism of $B_4C$ reinforced Mg-matrix composites fabricated by metal-assisted pressureless infiltration technique. *Trans. Nonferrous Met. Soci. China* 25 (8), 2543–2548. https://doi.org/10.1016/S1003-6326(15)63873-0.